JOURNAL OF AGRICULTURAL AND FOOD CHEMISTRY

ARTICLE

pubs.acs.org/JAFC

Fish Proteins as Targets of Ferrous-Catalyzed Oxidation: Identification of Protein Carbonyls by Fluorescent Labeling on Two-Dimensional Gels and MALDI-TOF/TOF Mass Spectrometry

Manuel Pazos,[*,†] Angela Pereira da Rocha,[§] Peter Roepstorff,[§] and Adelina Rogowska-Wrzesinska[§]

[†]Instituto de Investigaciones Marinas (IIM-CSIC), Eduardo Cabello 6, 36208 Vigo, Spain

[§]Department of Biochemistry and Molecular Biology, University of Southern Denmark, Campusvej 55, DK-5230 Odense, Denmark

ABSTRACT: Protein oxidation in fish meat is considered to affect negatively the muscle texture. An important source of free radicals taking part in this process is Fenton's reaction dependent on ferrous ions present in the tissue. The aim of this study was to investigate the susceptibility of cod muscle proteins in sarcoplasmic and myofibril fractions to in vitro metal-catalyzed oxidation and to point out protein candidates that might play a major role in the deterioration of fish quality. Extracted control proteins and proteins subjected to free radicals generated by Fe(II)/ascorbate mixture were labeled with fluorescein-5-thiosemicarbazide (FTSC) to tag carbonyl groups and separated by two-dimensional gel electrophoresis. Consecutive visualization of protein carbonyl levels by capturing the FTSC signal and total protein levels by capturing the SyproRuby staining signal allowed us to quantify the relative change in protein carbonyl levels corrected for changes in protein content. Proteins were identified using MALDI-TOF/TOF mass spectrometry and homology-based searches. The results show that freshly extracted cod muscle proteins exhibit a detectable carbonylation background and that the incubation with Fe(II)/ascorbate triggers a further oxidation of both sarcoplasmic and myofibril proteins. Different proteins exhibited various degrees of sensitivity to oxidation processes. Glyceraldehyde 3-phosphate dehydrogenase (GAPDH), nucleoside diphosphate kinase B (NDK), triosephosphate isomerase, phosphoglycerate mutase, lactate dehydrogenase, creatine kinase, and enolase were the sarcoplasmic proteins most vulnerable to ferrous-catalyzed oxidation. Moreover, NDK, phosphoglycerate mutase, and GAPDH were identified in several spots differing by their p*I*, and those forms showed different susceptibilities to metal-catalyzed oxidation, indicating that post-translational modifications may change the resistance of proteins to oxidative damage. The Fe(II)/ascorbate treatment significantly increased carbonylation of important structural proteins in fish muscle, mainly actin and myosin, and degradation products of those proteins were observed, some of them exhibiting increased carbonylation levels.

KEYWORDS: protein oxidation, protein carbonyls, metal-catalyzed protein oxidation, *Gadus morhua*, fluorescein-5-thiosemicarbazide (FTSC), MALDI-TOF/TOF, proteomics

INTRODUCTION

Protein oxidation is considered to be a deteriorative process in muscle-based foods during processing and storage, being mainly associated with discoloration and adverse textural changes such as loss of tenderness and juiciness.[1] Fish muscle is particularly prone to suffering oxidative deterioration due to its elevated proportion of highly oxidizable long-chain n-3 polyunsaturated fatty acids (PUFA), principally eicosapentaenoic acid (EPA, 20:5 n-3) and docosahexaenoic acid (DHA, 22:6 n-3).[2,3] Lipid peroxidation byproduct (free radicals, hydroperoxides, and aldehydes), redox active metals, and reactive oxygen species (hydroxyl radical, singlet oxygen, and hydrogen peroxide) are considered to be major promoters of the oxidative damage in proteins.[1,4]

Protein carbonylation is certainly the most employed marker of protein oxidation. Protein carbonyls can be formed directly by oxidation of the side chains of several amino acids, such as lysine, arginine, proline, and histidine, or by reaction of proteins with lipid oxidation products and advanced glycation end products, which can be attached to the proteins by Michael addition or Schiff base formation.[5−8] The reaction of protein carbonyls with 2,4-dinitrophenylhydrazine (DNPH) to form 2,4-dinitrophenylhydrazones (DNP) is a routine method for assessing protein oxidation. The direct measurement of the optical absorbance of DNP at 370 nm (ε = 22000 M^{-1} cm^{-1})[9] has a reduced sensitivity and reproducibility because of interferences from nonreacted DNPH or chromophores such as heme proteins and carotenoids.[10,11] Moreover, the colorimetric DNPH assay does not allow the individual identification of the oxidized proteins. Western blots directed to the protein−DNPH derivatives can solve these limitations in the analysis of protein carbonylation.[12] However, immunoblot-based procedures have disadvantages such as high cost and possible protein loss during protein transfer from the gel electrophoresis to the membrane and are time-consuming. Recently, alternative methodologies derived from avidin/biotin affinity,[13,14] derivatization with Girard P reagent,[15] and labeling with fluorescein-5-thiosemicarbazide (FTSC)[16] have been successfully combined with proteomic techniques to identify carbonylated proteins in biological samples.

Nowadays, many of the investigations still employ the direct spectrophotometric measurement of protein−DNPH derivatives to assess protein oxidation in meat-based foods.[17−19] More

Received: March 16, 2011
Revised: May 26, 2011
Accepted: June 1, 2011
Published: June 01, 2011

advanced procedures based on Western blotting directed to protein−DNPH derivatives have been attempted to identify specific carbonylated proteins in chicken meat,[20] lamb meat,[21] and fish muscle.[22−24] Recently, fluorescent labeling combined with gel electrophoresis has also been successfully used to detect carbonylated proteins in fish muscle.[25] However, despite all efforts focused on understanding protein oxidation in meat-based foods, important aspects about the mechanisms of the oxidative degradation of proteins and their implication on meat quality remain to be elucidated.[26] More studies are also needed to identify the role of lipid−protein interactions in the protein oxidation processes, as well as to characterize the principal catalysts of protein oxidation in meat. The incorporation of recent technical advances in proteomic tools in the field of food science is proposed to generate valuable high-throughput data that reveal both the pathways of protein oxidation and effective inhibitory treatments in meat-based foods.

The aim of the present study was to investigate the susceptibility of fish proteins to metal-catalyzed oxidation (MCO). With this purpose, isolated sarcoplasmic and myofibril proteins from cod (*Gadus morhua*) muscle were individually treated with an iron(II)/ascorbate oxidation generating system. The carbonylation level of proteins subjected to MCO and control proteins (nontreated) was monitored by derivatization of carbonyl groups with FTSC. FTSC labeling allows visualization and quantification of the relative amount of protein carbonyls on gels by fluorescent detection and optical density measurements. Proteins were separated using two-dimensional gel electrophoresis (2-DE) and identified using matrix-assisted laser desorption−ionization time-of-flight (MALDI-TOF/TOF) mass spectrometry.

MATERIALS AND METHODS

Materials. Fresh Atlantic cod (*G. morhua*) was obtained from a local market and directly transported on ice to the laboratory. FTSC and Sypro Ruby protein gel stain were purchased from Molecular Probes (Junction City, OR). Protease inhibitor cocktail tablets were from Roche (Mannheim, Germany). Dithiothreitol (DTT), trichloroacetic acid (TCA), Tris-HCl, 3,3-cholaminopropyldimethylammonio-1-propanesulfonate (CHAPS) were purchased from Sigma (St. Louis, MO). Urea and thiourea were respectively obtained from ICN Biomedicals (Irvine, CA) and Fluka (Buchs, Switzerland). Sodium dodecyl sulfate (SDS) and Serdolit MB-1 were from Serva (Heidelberg, Germany). Glycerol was obtained from Merck (Darmstadt, Germany). Immobilized pH-gradient strips covering pH 3−11 NL (18 cm), Pharmalyte 3−10, and deStreak reagent were purchased from GE Healthcare Science (Uppsala, Sweden). Forty percent acrylamide and 2% bis(*N*,*N*′-methylene)-bis(acrylamide) were from Bio-Rad (Hercules, CA). All other chemicals were of reagent/analytical grade, and water was purified using a Milli-Q system (Millipore, Billerica, MA).

Extraction of Sarcoplasmic and Myofibril Proteins. Sarcoplasmic (low-salt-soluble) and myofibril (high-salt-soluble) proteins were isolated from cod light muscle. For this purpose, light muscle was minced and homogenized with 5 volumes of 10 mM Tris-HCl, pH 7.2, using an Ultra-Turrax high-performance disperser. The homogenate was centrifuged at 5000*g* (4 °C, 15 min). The supernatant was used to obtain sarcoplamic proteins, and the pellet was employed to prepare the myofibril protein fraction. The sarcoplasmic fraction was further centrifuged at 130000*g* (4 °C, 30 min), and the supernatant was collected, whereas the pellet, composed of phospholipids and other membrane components, was discarded. The myofibril proteins were isolated by homogenizing the pellet from the first centrifugation with a saline solution (0.6 M NaCl, 10 mM Tris buffer, pH 7.2) and collecting the supernatant obtained after centrifugation at 4500*g* (4 °C, 15 min). Sarcoplasmic and myofibril fractions were stored in the presence of a protease inhibitor cocktail at −80 °C until use. The concentration of protein was measured by using the Bradford assay.[27]

Metal-Catalyzed Oxidation of Protein Fractions and FTSC Labeling of Protein Carbonyls. Carbonyl residues on proteins were activated via a metal-catalyzed reaction with Fe(II) and ascorbate. Protein fractions (final concentration = 2.5 mg of protein/mL) were treated with $FeCl_2 \cdot 4H_2O$ (24 μM) and sodium ascorbate (6 mM) in a buffer solution containing 50 mM Hepes, pH 6.0, 100 mM $MgCl_2$, 100 mM KCl, and 3 M guanidine. The samples were incubated for 2 h in the dark at room temperature. To stop the oxidation reaction, 3 μL of EDTA (0.25 M) was added to 600 μL of protein solution (2.5 mg/mL). The labeling and washing of protein carbonyls was performed by following a published protocol.[16] Proteins were incubated with 1 mM FTSC at 37 °C for 2 h and 15 min in the dark. The proteins were then precipitated with an equal volume of 20% chilled TCA and centrifuged at 16000*g* (25 °C, 5 min). The pellets were washed five times with ethanol/ethyl acetate (1:1), and the final pellets were dissolved in urea buffer (7 M urea, 2 M thiourea, 2% CHAPS, 0.4% DTT, 0.5% Pharmalyte 3−10, and 0.5% IPG 3−10 buffer). Protein concentration was measured by using the Bradford assay.[27]

2-D Gel Electrophoresis. Isoelectric focusing and 2-DE were performed as described before.[28] Briefly, approximately 500 μg of proteins was applied to IPG 3−11 NL strips by reswelling overnight with a final volume of 300 μL per gel. Focusing on IPG strips was performed on a Multiphor II electrophoresis unit (GE Healthcare Science, Uppsala, Sweden) at 20 °C using a voltage/time profile linearly increasing from 0 to 600 V for 2 h and 15 min, from 600 to 3500 V for 4 h, and at 3500 V for 1 h and 28 min. After focusing, strips were equilibrated twice for 15 min in equilibration buffer (6 M urea, 2% SDS, 30% glycerol, 50 mM Tris-HCl, pH 8.8, 1% DTT). For convenience, the strips were kept frozen at −80 °C between the two equilibration steps.

SDS-PAGE second-dimension gel electrophoresis was performed using a vertical Protean II System (Bio-Rad Laboratories) and laboratory-made 12.5% (w/v) acrylamide gels (acrylamide:*N*,*N*′-ethylene-bis(acrylamide) ratio 200:1). The gels were run overnight at a constant current setting (6 mA/gel for 2 h and 10 mA/gel for approximately 16 h) at 20 °C. The running buffer was an aqueous solution composed of 0.67% (w/v) Tris-base, 1.44% glycine, and 0.1% SDS. After gel electrophoresis, the gels were fixed with 45% methanol and 7.5% acetic acid (1 h, at room temperature) and scanned using a Typhoon 9400 scanner (Amersham Biosciences, Uppsala, Sweden) using blue excitation mode (488 nm) and an 520 nm band-pass filter (520 BP 40). After the fluorescence signal from FTSC residues in the proteins had been measured, the gels were stained for 3 h with Sypro Ruby dye to visualize the total protein content. The fluorescence image scanner Typhoon 9400 was set to green excitation mode (532 nm), and an emission band-pass filter of 610 nm (610 BP 30) was used to scan the Sypro Ruby-associated fluorescence on gels.

In-Gel Digestion of Protein Spots. Spots containing the proteins of interest were manually excised from gels and were washed first with deionized water and then with 100% acetonitrile for 5 and 15 min, respectively. This washing step was repeated twice. The gel plugs were dehydrated in a vacuum centrifuge and rehydrated with a solution of 2% trypsin (Promega Inc., Madison, WI) in 50 mM NH_4HCO_3, at 4 °C. After 20 min, the excess trypsin solution was removed, 30 μL of 50 mM NH_4HCO_3 was added, and digestion proceeded at 37 °C overnight, followed by storage at −20 °C until use. Peptide desalting was performed on custom-made reverse-phase microcolumns, prepared with R2 resin (Perseptive Biosystems Inc., Framingham, MA) as described elsewhere.[29] The peptide solution, obtained from digestion of each spot, was loaded onto the microcolumn, followed by washing with 10 μL of 1% trifluoroacetic acid (TFA). Bound peptides were eluted with

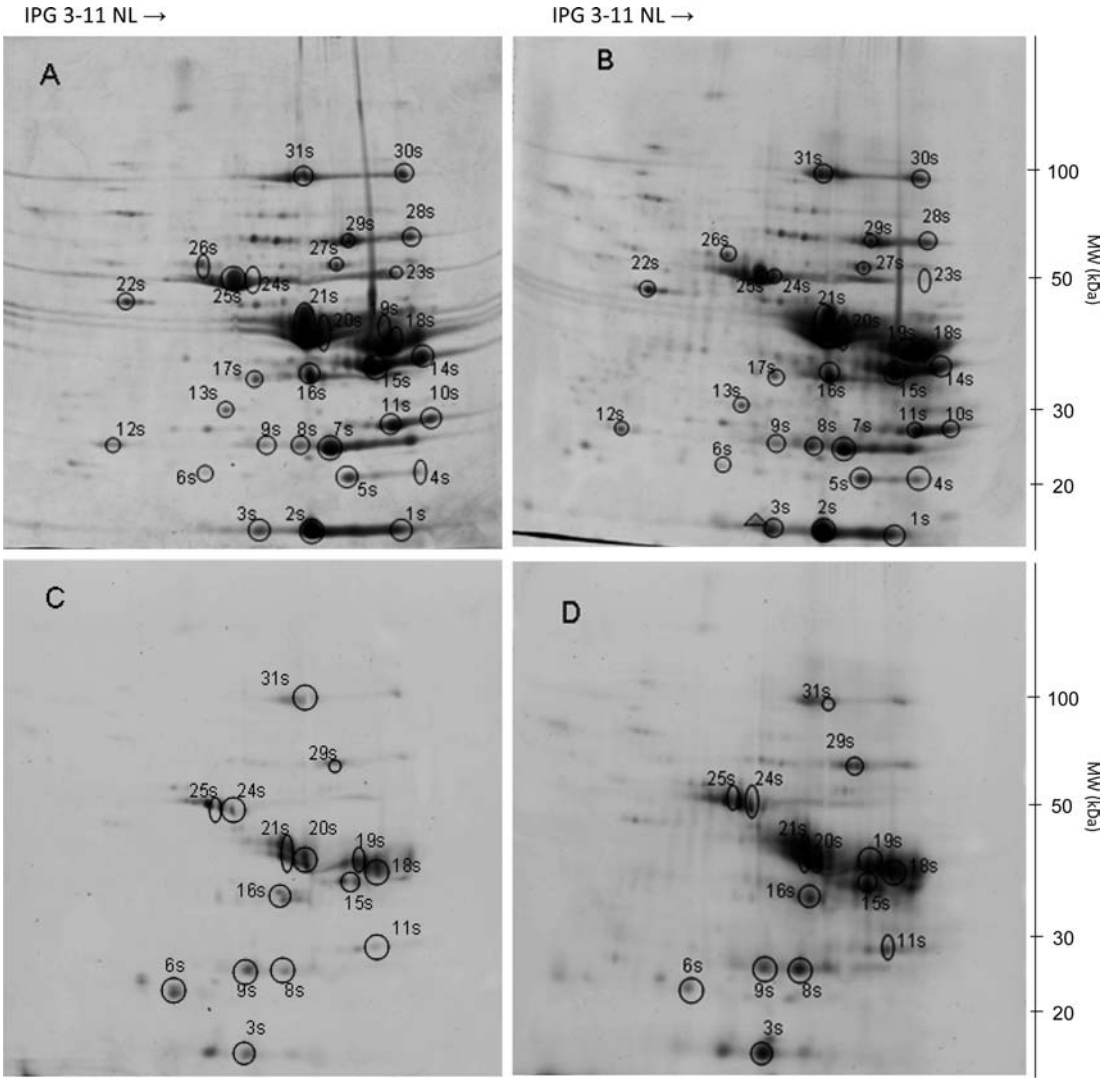

Figure 1. 2-DE of cod sarcoplasmic proteins. Images were visualized by total protein stain (Sypro Ruby) to show the protein pattern of nonoxidized sarcoplasmic proteins (A) and those subjected to ferrous-catalyzed oxidation (B). Protein carbonyls were visualized by the FTSC staining of identical gels of nonoxidized sarcoplasmic proteins (C) and those subjected to ferrous-catalyzed oxidation (D). Proteins were separated using IPG 3−11 NL gels in the first dimension (horizontal) and 12.5% polyacrylamide gels in the second dimension (vertical). Circles and numbers indicate proteins that have been identified by MALDI-MS/MS and are listed in Table 1.

0.8 μL of matrix solution (5 μg/μL of α-cyano-4-hydrocinnamic acid in 70% acetonitrile and 0.1% TFA) directly onto the matrix-assisted laser desorption ionization (MALDI) target plate. Peptide mass spectra were acquired in positive reflector mode on a 4700 Plus MALDI TOF/TOF Analyzer (Applied Biosystems, Foster City, CA) using 20 kV of acceleration voltage. Each spectrum was obtained with a total of 800 laser shots and was externally calibrated using peptides derived by tryptic digestion of β-lactoglobulin. Tandem mass spectra were acquired using the same instrument in MS/MS positive mode. From the raw data output, peak lists were generated by Data Explorer (Applied Biosystems). MS and MS/MS peak lists were combined into search files and used to search NCBI databases using the Mascot search engine (Matrix Science Ltd., London, U.K.). Search parameters were as follows: database, NCBInr version 20100602; taxonomy, vertebrates; enzyme, trypsin; allow up to 1 missed cleavage; fixed modifications, none; variable modifications, methionine oxidation; peptide mass tolerance, 70 ppm; and fragment mass tolerance, 500 ppm. If the spectrum clearly indicated the presence of peptides (contained at least three intense peaks) and no protein was found matching the spectrum, the remaining sample was derivatized by adding 7 μL of 10 μg/μL of 4-sulfophenyl isothiocyanate dissolved in 20 mM $NaHCO_3$, pH 8.6. The reaction was carried out for 30 min at 50 °C and terminated using 1 μL of 1% TFA. The mixture was then loaded on the chromatographic column (as described above), eluted on the target, and analyzed on a 4800 Proteomics Analyzer (Applied Biosystems). Derivatized peptides (showing a mass difference of 215 Da compared to the original MS spectra) were sequenced using air as a collision gas. The obtained spectra of fragment ions were analyzed either manually or using the AminoCalc program (Protana A/S, Denmark) to find the distance between fragment ions and the amino acid sequences. The obtained sequences were used to search the NCBI protein database using MS BLAST Search at EMBL.[30]

Image Analysis. 2-DE protein patterns were analyzed by using PDQuest software version 7.1 (Bio-Rad) to locate and match the protein spots among the gels. Protein quantities or carbonylation levels were expressed as parts per million (ppm) of the total integrated optical density of each gel. To quantify the observed changes in protein species abundance and protein carbonylation between oxidized and nonoxidized protein fractions, we have calculated three different parameters:

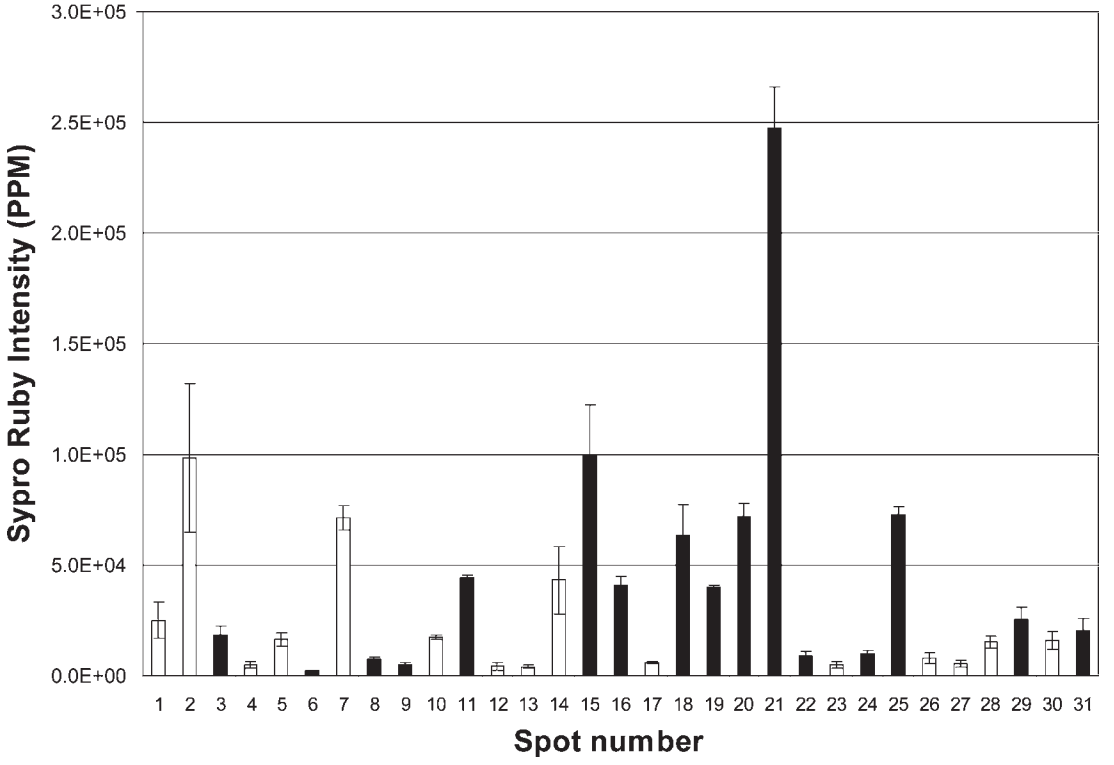

Figure 2. Relationship between the abundance of cod sarcoplasmic proteins and their susceptibility to ferrous-catalyzed oxidation. Bar heights indicate the relative concentration of each protein based on the intensity of the Sypro Ruby staining. Proteins with detectable carbonylation levels in the absence/presence of the oxidizing system are shown as black bars, whereas proteins without significant oxidation are shown as white bars.

protein fold, oxidation fold, and oxidation index. Protein folds have been calculated from the Sypro Ruby gels by dividing protein abundance observed in oxidized and nonoxidized protein fractions and characterize the change in the protein species content before and after oxidation. Oxidation folds have been obtained from FTSC-stained gels by dividing levels of protein carbonyls observed in oxidized and nonoxidized samples and describe the change in protein carbonylation between those samples. Finally, oxidation index has been calculated by normalizing the increase in protein carbonyl content (oxidation fold) to the corresponding increase in protein content (protein fold). Some protein spots were present only in one of the analyzed conditions. To calculate the protein folds for those protein spots we have included "empty" spots copied from the Sypro Ruby protein pattern where the spot was visible over to the other one, thus including gel background in the calculation, which is a widely accepted practice in 2-DE image analysis. The oxidation folds were calculated in a similar way when protein oxidation was not observed in control samples. Oxidation fold was then the rate between the FTSC signal of the Fe(II)/ascorbate-treated proteins and the FTSC background of the control samples.

Statistical Analysis. The experiments were performed twice, and all types of samples (treated and not treated with MCO) were prepared in triplicate and run in three different 2-DE gels. The mean and standard deviation were calculated, and statistical significance was assessed using a one-tailed Student's t test among three independent replicates ($n = 3$). Differences were considered to be significant at a critical p value of <0.05. Statistical analyses were performed using Statistica 6.0 software (Statsoft Inc., Tulsa, OK).

RESULTS AND DISCUSSION

The vulnerability of sarcoplasmic and myofibril proteins from cod skeletal muscle to metal -catalyzed oxidation was evaluated by comparing carbonyl levels in isolated muscle protein fractions treated with a continuous source of ferrous ions from the Fe(II)/ascorbate system with control protein fractions not subjected to metal-catalyzed oxidation. Protein carbonylation was detected on 2-DE gels by FTSC staining that labels the carbonyl residues with fluorescence in a quantitative manner.[16] The protein spots of interest were identified by protein fingerprints (PMF) and peptide sequencing (MS/MS) using MALDI-TOF/TOF mass spectrometry.

Protein Oxidation in the Sarcoplasmic Protein Fraction. Ferrous ions can promote oxidation through a Fenton-type mechanism to produce highly reactive hydroxyl radicals ($^{-\bullet}OH$) by reaction with hydrogen peroxide (H_2O_2).[31] Ferrous ions may also participate in the formation of H_2O_2, because they can react with molecular oxygen to generate superoxide radicals ($O_2^{\bullet-}$), which develop dismutation to generate H_2O_2.[31] These reactions transform ferrous ions to ferric ions, which are recycled to the former ferrous state by the reducing ascorbate.

The incubation of sarcoplasmic proteins with the Fe(II)/ascorbate-based oxidation generating system provoked few changes in the 2-DE pattern of proteins as visualized by Sypro Ruby staining (Figure 1). An additional spot (marked with a triangle in Figure 1B) was found next to one assigned to nucleoside diphosphate kinase B (spot 3s) in the oxidized sarcoplasmic fraction. This new spot was also observed on the 2-D gel pattern of the oxidized myofibril proteins (protein spot 29m), being identified as a fragment of the nucleoside diphosphate kinase B (Figure 2B). Moreover, incubation of proteins with the Fe(II)/ascorbate-based oxidation generating system altered the abundance level of seven protein spots. Protein spots 3s and 8s, identified respectively as nucleoside diphosphate kinase B and

Table 1. Proteins Identified from the 2-DE Map of the Sarcoplasmic Protein Fraction from Cod Muscle[a]

spot no.	identification	species	NCBI accession no.	identification method	no. of matching peptides MS/(MS/MS)	coverage (%)	sequenced peptides	score	MWt/ MWe (kDa)	pIt/pIe
1s	nucleoside diphosphate kinase B	*Merluccius capensis*	gi|158705971	PMF + MS/MS	2/2	23	-.TFVAIKPDGVQR.G K. MMLGETNPADSKPGSIR.G	147	14.2/14.2	5.7/7.9
2s	nucleoside diphosphate kinase B	*Merluccius capensis*	gi|158705971	PMF + MS/MS	2/1	23	-.TFVAIKPDGVQR.G	77	14.2/14.4	5.7/6.5
3s	nucleoside diphosphate kinase B	*Merluccius capensis*	gi|158705971	PMF + MS/MS	2/2	23	-.TFVAIKPDGVQR.G K.MMLGETNPADSKPGSIR.G	190	14.2/14.5	5.7/6.1
4s	adenylate kinase 1-2	*Epinephelus coioides*	gi|222088001	PMF + MS/MS	13/5	37	K.IIFWGGPGSGK.G K.GELVPLDTVLDMIK.D K.RLDLVYK.A K.ATEPVIAFVEGR.G K.YGYTHLSSGDLLR.A	241	21.2/20.2	7.6/8.3
5s	adenylate kinase 1-2	*Epinephelus coioides*	gi|222088001	PMF + MS/MS	13/5	37	K.IIFWGGPGSGK.G K.GELVPLDTVLDMIK.D K.RLDLVYK.A K.ATEPVIAFVEGR.G K.YGYTHLSSGDLLR.A	320	21.2/20.2	7.6/7.2
6s	peroxiredoxin-1	*Salmo salar*	gi|213512853	PMF + MS/MS	3/3	I8	R.DYGVLKEDQGIAYR.G R.GLFVIDDKGILR.Q R.QITINDLPVGR.S	196	21.9/21.6	5.6/5.8
7s	triosephosphate isomerase	*Esox lucius*	gi|225716614	PMF + MS/MS	6/1	26	K.VVLAYEPVWAIGTGK.T	85	29.6/24.0	8.2/7.0
8s	triosephosphate isomerase B	*Danio rerio*	gi|47271422	PMF + MS/MS	10/4	21	K.GAFTGEISPAMIK.D R.RHVFGESDELIGQK.V R.HVFGESDELIGQK.V K.TNVSEAVANSVR.I	214	26.8/24.7	6.9/6.4
9s	triosephosphate isomerase B	*Danio rerio*	gi|47271422	PMF + MS/MS	7/3	18	K.GAFTGEISPAMIK.D R.HVFGESDELIGQK.V K.TNVSEAVANSVR.I	164	26.8/25.1	6.9/6.2
10s	phosphoglycerate mutase 2-2	*Salmo salar*	gi|213515184	PMF + MS/MS	5/1	12	K.NVIIAAHGNSLR.G	114	28.6/28.6	8.9/8.9
	phosphoglycerate mutase 2-1		gi|213515006							
11s	phosphoglycerate mutase 2-1	*Salmo salar*	gi|213515184	PMF + MS/MS	5/2	12	R.ALPYWNDVIAPEIK.A	134	28.6/28.1	8.9/8.4
	phosphoglycerate mutase 2-1		gi|213515006				K.NVIIAAHGNSLR.G			
12s	preproapolipoprotein A-I	*Gadus morhua*	gi|52783666	PMF + MS/MS	7/3	49	R.SAVGMYLDQVKDSAAR.S K.AQLATSLDSLQASIK.T K.TAQAGAEPYTDAAVAQV-MEATTEVR.A	198	14.8/26.9	5.9/4.8
13s	guanidinoacetate *N*-methyltransferase	*Danio rerio*	gi|157743330	PMF + MS/MS	5/1	12	R.VLEIGFGMAIAATK.V	90	26.7/30.1	5.9/5.9

dx.doi.org/10.1021/jf201080t |*J. Agric. Food Chem.* 2011, 59, 7962–7977

Table 1. Continued

spot no.	identification	species	NCBI accession no.	identification method	no. of matching peptides MS/(MS/MS)	coverage (%)	sequenced peptides	score	MWt/ MWe (kDa)	pIt/pIe
14s	glyceraldehyde 3-phosphate dehydrogenase	*Gadus morhua*	gi|25989185	PMF + MS/MS	18/5	57	K.VIHDNFGIVEGLMS-TVHAITATQK.T R.VPTPNVSVVDLTVR.L K.GILGYTEDQVVSTDFNGDIR.S R.SSIFDAGAGIALNDHFVK.L K.LVTWYDNEFGYSNR.V	500	36.1/34.0	7.7/8.7
15s	glyceraldehyde 3-phosphate dehydrogenase	*Gadus morhua*	gi|25989185	PMF + MS/MS	17/6	36	K.VIHDNFGIVEGLMSTV-HAITATQK.T K.ITGMAFRVPTPNVSVVDLTVR.L R.VPTPNVSVVDLTVR.L R.VPTPNVSVVDLTVRLEKPAK.Y R.SSIFDAGAGIALNDHFVK.L K.LVTWYDNEFGYSNR.V	362	36.1/33.5	7.7/7.9
16s	lactate dehydrogenase A chain	*Notothenia neglecta*	gi|17433116	PMF + MS/MS	9/4	17	K.VTVVGVGMVGMASAVSILLK.D K.LKGEVMDLQHGSLFLK.T K.GEVMDLQHGSLFLK.T K.FIIPNIVK.Y	152	36.1/33.0	6.7/6.6
17s	glyceraldehyde 3-phosphate dehydrogenase	*Rachycentroncanadum*	gi|226524991	PMF + MS/MS	4/2	7	K.GADILIFVVPHQFIVR.V R.LGLMEMIAFAK.V	76	38.1/33.2	6.3/6.15
18s	creatine kinase	*Gadus morhua*	gi|13274539	PMF + MS/MS	11/5	33	K.LSTHAKFEEILTR.L K.LSIEALATLSGEFK.G K.RGTGGVDTASVGGVFD-ISNADR.L R.GTGGVDTASVGGVFDISNADR.L R.LGSSEVDQVQMVVDGVK.L	407	28.9/35.6	8.9/8.4
19s	creatine kinase muscle isoform 2	*Chaenocephalus aceratus*	gi|31322099	PMF + MS/MS	10/4	18	K.LSVEALTSLDGEFK.G R.LGSSEVAQVQLVVDGVK.L R.GTGGVDTASVGGVFDISNADR.L K.RGTGGVDTASVGGVFDISNADR.L	184	42.7/36.1	6.4/7.9
20s	creatine kinase	*Gadus morhua*	gi|13274539	PMF + MS/MS	13/3	34	K.GFTLPPHNSR.G K.LSIEALATLSGEFK.G K.LSIEALATLSGEFKGK.Y	256	28.9/38.0	8.9/6.8
21s	creatine kinase-3	*Salmo salar*	gi|1197632335	PMF + MS/MS	7/2	14	R.LSVEALDTLDGEFKGK.Y R.GTGGVDTASVGGVFDISNADR.L	93	42.9/33.4	6.3/6.5

dx.doi.org/10.1021/jf201080t |J. Agric. Food Chem. 2011, 59, 7962–7977

Table 1. Continued

spot no.	identification	species	NCBI accession no.	identification method	no. of matching peptides MS/(MS/MS)	coverage (%)	sequenced peptides	score	MWt/ MWe (kDa)	pIt/pIe
22s	actin, aortic mooth muscle	*Danio reno*	gi|197632385	PMF + MS/MS	12/3	31	R.AVFPSIVGRPR.H K.SYELPDGQVITIGNER.F R.VAPEEHPTLLTEAPLNPK.A	263	42.1/42.0	5.2/5.2
23s	enolase 3-1	*Salmo salar*	gi|213511756	PMF + MS/MS	4/2	9	R.IGAEVYHNLKNVIK.A R.AAVPSGASTGIHEALELR.D	128	47.2/47.5	6.8/8.4
24s	unnamed protein product	*Tetraodon nigroviridis*	gi|147210809	PMF + MS/MS	6/1	16	K.AGYPDKIIIGMDVAASEFYR.S	74	47.1/48.0	6.0/6.1
25s	β-enolase-1	*Chiloscyllium punctatum*	gi|11999263	PMF + MS/MS	2/1	15	R.HIADLAGNKDNVLPVPAFNV-INGGSHAGNK.L	62	39.4/48.8	5.9/6.0
26s	enolase A	*Acipenser baerii*	gi|98979415	PMF + MS/MS	11/4	23	R.IGAEVYHNLK.N K.IVIGMDVAASEFYK.D R.AAVPSGASTGIYEALELR.D K.LAMQEFMILPVGASSFK.D	297	47.1/54.5	6.0/5.8
27s	phosphoglucose isomerase-2	*Mugil cephalus*	gi|20067651	PMF + MS/MS	6/1	17	K.TLAQLNAETTLFIIASK.T	81	62.1/51.0	7.8/7.3
28s	pyruvate kinase	*Salmo salar*	gi|213512270	PMF + MS/MS	9/2	15	R.RFDEILEASDGIMVAR.G K.DIQDLQFGVEQGVDMVF-ASFIR.K	103	58.3/61.4	8.2/8.4
29s	pyruvate kinase	*Salmo salar*	gi|213512270	PMF + MS/MS	11/2	16	R.RFDEILEASDGIMVAR.G K.DIQDLQFGVEQGVDMVF-ASFIR.K	225	58.3/60.9	8.2/7.5
30s	glycogen phosphorylase, muscle form	*Salmo salar*	gi|213515556	PMF + MS/MS	17/3	18	R.IGEEFVR.D K.VIFLENYR.V R.DYYFALANTVR.D	216	97.4/95.9	6.7/8.3
31s	unnamed protein product (similar to glycogen phosphorylase)	*Tetraodon nigroviridis*	gi|47227171	PMF + MS/MS	18/3	19	R.LKQEYFVVSATLQDIIR.R R.IGEDFIR.D K.VIFLENYR.V	299	97.2/97.0	6.5/6.3

[a] Spots of interest were identified by MS as described under Materials and Methods. Protein spot numbers refer to numbered spots on Figure 1. For each spot, different parameters supporting the protein identification by MS are indicated (accession number; identification method (PMF, protein mass fingerprint; or MS/MS, protein sequencing); number of matching peptides in MS mode (finger printing) and MS/MS mode (sequencing); % sequence coverage; sequence of sequenced peptides, Mascot score, theoretical and experimental protein mass (MWt and MWe), theoretical and experimental protein isoelectric point (pIt and pIe).

dx.doi.org/10.1021/jf201080t |J. Agric. Food Chem. 2011, 59, 7962–7977

Table 2. Quantification of Changes in Protein Species Content and Carbonylation Level as a Consequence of the Incubation of the Sarcoplasmic Protein Fraction to Ferrous-Catalyzed Oxidation

spot no.	identification	NCBI accession no.	protein fold[a,b]	oxidation fold[b,c]	oxidation index[d]
3s	nucleoside diphosphate kinase B	gi|158705971	1.77 ± 0.08**	3.70 ± 0.35**	2.10
6s	peroxiredoxin-1	gi|213512853	0.97 ± 0.31	0.23 ± 0.04*	0.24
7s	triosephosphate isomerase	gi|225716614	0.90 ± 0.06	2.02 ± 0.38*	2.25
8s	triosephosphate isomerase B	gi|47271422	2.48 ± 0.34**	3.30 ± 0.03***	1.33
9s	triosephosphate isomerase B	gi|47271422	1.01 ± 0.11	0.59 ± 0.17	0.58
11s	phosphoglycerate mutase 2-2	gi|213515184	0.53 ± 0.02***	1.76 ± 0.28	3.34
	phosphoglycerate mutase 2-1	gi|213515006			
15s	glyceraldehyde 3-phosphate dehydrogenase	gi|25989185	1.00 ± 0.33	4.75 ± 1.02**	4.76
16s	lactate dehydrogenase A chain	gi|17433116	0.93 ± 0.05	2.71 ± 0.26**	2.93
18s	creatine kinase	gi|13274539	1.05 ± 0.11	2.35 ± 0.22*	2.24
19s	creatine kinase muscle isoform 2	gi|31322099	1.24 ± 0.15	0.83 ± 0.08	0.67
20s	creatine kinase	gi|13274539	1.34 ± 0.11*	2.18 ± 0.22**	1.62
21s	creatine kinase-3	gi|197632385	0.97 ± 0.02	2.12 ± 0.07***	2.19
22s	actin, aortic smooth muscle	gi|47086797	1.44 ± 0.14*	1.61 ± 0.36*	1.12
24s	unnamed protein product	gi|47210809	1.63 ± 0.25*	1.80 ± 0.21*	1.10
25s	β-enolase-1	gi|11999263	0.82 ± 0.09*	2.27 ± 0.53*	2.78
29s	pyruvate kinase	gi|213512270	0.69 ± 0.27	1.18 ± 0.26	1.72
31s	unnamed protein product (similar to glycogen phosphorylase)	gi|47227171	0.84 ± 0.33	1.46 ± 0.74	1.71

[a] Protein fold between sarcoplasmic proteins subjected to ferrous-catalyzed oxidation and those not incubated with ferrous (controls) are calculated from quantification from the Sypro Ruby-stained 2-DE gels. [b] Protein carbonylation levels between ferrous-treated sarcoplasmic proteins and those not treated (controls) were found to be significantly different at <0.05 (*), <0.005 (**), or <0.0005) (***). [c] Oxidation fold between sarcoplasmic proteins subjected to ferrous-catalyzed oxidation and those not incubated with ferrous (controls) are calculated from quantification of FTSC-stained 2-DE gels. [d] Oxidation indices correspond to the oxidation fold normalized to the corresponding protein fold.

triosephosphate isomerase, showed a significant ($p < 0.005$) overexpression in oxidized samples (Table 2). The intensities of protein spots 20s (creatine kinase), 22s (actin), and 24s (unnamed protein product) also increased significantly ($p < 0.05$). In contrast, the content of protein spots 11s (phosphoglycerate mutase) and 25s (β-enolase-1) decreased after oxidation.

FTSC-stained 2-D gels showed a low degree of carbonylation in sarcoplasmic proteins in control protein fractions (Figure 1C). Detectable levels of carbonylation were observed for proteins identified as nucleoside diphosphate kinase B (spot 3s), peroxiredoxin-1 (spot 6s), triosephosphate isomerase (spots 8s and 9s), phosphoglycerate mutase (spot 11), glyceraldehyde 3-phosphate dehydrogenase (spot 15s), lactate dehydrogenase A chain (spot 16s), creatine kinase (spots 18s, 19s, 20s, and 21s), actin (spot 22s), unnamed protein product (spot 24s), β-enolase-1 (spot 25s), pyruvate kinase (spot 29s), and an unnamed protein product similar to glycogen phosphorylase (spot 31s) (Figure 1C and Table 1). The elevated level of carbonyl groups detected in the control samples of some low abundant proteins is noteworthy, for example, spots 3s (nucleoside diphosphate kinase B isoform), 6s (peroxiredoxin-1), 8s (triosephosphate isomerase B \ sarcoplasmic proteins also revealed the lack of carbonylation in several high abundant proteins, as in the case of protein spots assigned to nucleoside diphosphate kinase B (spot 2s), triosephosphate isomerase (spots 7s), and glyceraldehyde 3-phosphate dehydrogenase (spot 14s) (Figures 1C and 2). Therefore, the susceptibility of several sarcoplasmic proteins from cod that have a considerable background of carbonyl groups even under nonoxidizing conditions does not appear to be concentration-dependent. Kjaersgard et al.[22,24] have reported important levels of protein carbonyls in the sarcoplasmic and the total protein fraction of fresh rainbow trout muscle tissues, and those basal contents of protein carbonyls were found to be increased during storage. Kinoshita et al.[25] have also observed an important increment of protein carbonylation level during the storage of bonito muscle tissue.

The incubation of the sarcoplasmic fraction with the Fe(II)/ascorbate-based oxidation generating system significantly increased carbonylation for some of the detected proteins (Figure 1D). Previous investigations have described the formation of protein carbonyls under exposure to MCO in bovine serum albumin (BSA)[32] and in numerous cytosolic proteins from liver tissue[16] and have reported a high correlation between the iron content and the extent of protein oxidation.[33] The image analysis of FTSC-stained 2-DE gels by the software PDQuest allowed us to measure the optical density of all the spots detected and was used to quantify the changes in the protein abundance and oxidation levels. The observed changes were expressed as protein fold, the change in the total protein content before and after oxidation; oxidation fold, the change in protein carbonylation between those samples; and oxidation index, calculated by normalizing the increase in protein carbonyl content (oxidation fold) to the corresponding increase in protein content (protein fold) (Table 2). The incubation of the sarcoplasmic fraction with the Fe(II)/ascorbate-based oxidation generating system provoked the highest increment of carbonylation (4.75-fold) between treated and nontreated samples for protein spot 15s (glyceraldehyde 3-phosphate dehydrogenase) (Table 2). The highest observed oxidation index in this study clearly indicates that glyceraldehyde 3-phosphate dehydrogenase is highly susceptible to MCO. Isoforms corresponding to nucleoside diphosphate kinase B (spot 3s) and triosephosphate isomerase (spot 8s)

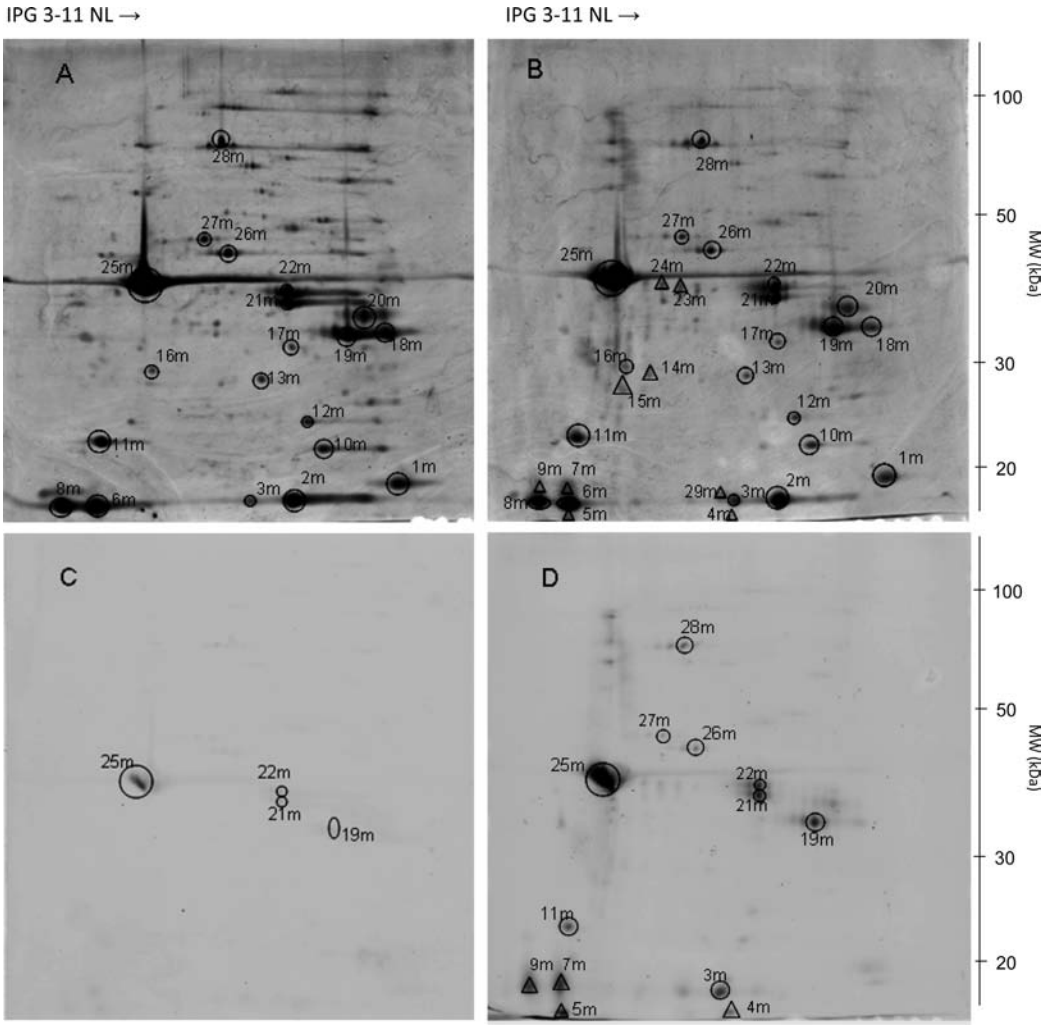

Figure 3. 2-DE of cod myofibril proteins. Images were visualized by total protein stain (Sypro Ruby) to show the protein pattern of nonoxidized myofibril proteins (A) and those subjected to ferrous-catalyzed oxidation (B). Protein carbonyls were visualized by the FTSC staining of identical gels of nonoxidized myofibril proteins (C) and those subjected to ferrous-catalyzed oxidation (D). Proteins were separated using IPG 3−11 NL gels in the first dimension (horizontal) and 12.5% polyacrylamide gels in the second dimension (vertical). Circles and numbers indicate proteins that have been identified by MALDI-TOF/TOF mass spectrometry and are listed in Table 2.

showed also an important increment (3.3−3.7-fold) in the carbonylation levels. The oxidation was not as increased (2−3-fold) for other isoforms of triosephosphate isomerase (spot 7s), lactate dehydrogenase (spot 16s), creatine kinase (spots 18s, 20s, and 21s) and enolase-1 (spot 25s), although these proteins also exhibited a high oxidation index (2.10−3.34), which confirms their vulnerability to MCO. The exception is protein spot 8s, which showed an oxidation index of 1.33 related to its much higher content (approximately 2.5-fold) in oxidized samples. Peroxiredoxin-1 was the only protein spot that showed significantly decreased carbonylation levels in oxidized samples (Table 2). The results also revealed proteins highly resistant to MCO. Proteins in spots 2s (nucleoside diphosphate kinase B isoform), 7s (triosephosphate isomerase isoform), and 14s (glyceraldehyde 3-phosphate dehydrogenase) did not exhibit detectable carbonylation under the treatment of the Fe(II)/ascorbate-based oxidation generating system despite their relatively high abundance (Figure 1D).

A remarkable finding was the isoform-dependent behavior of the proteins. In our study, we observed different oxidative susceptibilities of isoforms from nucleoside diphosphate kinase B (spots 1s, 2s, and 3s), phosphoglycerate mutase (spots 10s and 11s), and glyceraldehyde 3-phosphate dehydrogenase (spot 14s and 15s) (Figure 1 and Table 2). NDK exchanges phosphate groups among different nucleoside diphosphates. Phosphoglycerate mutase is a glycolytic transferase enzyme that catalyzes the conversion of 3-phosphoglycerate (PG) into 2-PG. Glyceraldehyde 3-phosphate dehydrogenase (GAPDH) is an important glycolytic enzyme that transfers a phosphate group to the glyceraldehyde 3-phosphate. All of these proteins have in common that they display different phosphorylation states, which could explain the differences in isoelectric point between the different spots observed. Phosphorylation results in a more acidic isoelectric point. In the case of NDK B, the isoform 3s with a lower isoelectric point showed higher carbonyl levels under Fe(II)/ascorbate treatment than the most abundant isoforms with higher isoelectric point, spots 1s and 2s. Phosphate groups are potential binding sites for metal ions; thus, phosphorylation might favor MCO by facilitating a closer contact between the pro-oxidant agent and the protein. A similar reasoning can be employed to

Table 3. Proteins Identified from the 2-DE Gels of the Myofibril Protein Fraction from Cod Muscle[a]

spot no.	identification	species	NCBI accession no.	identification method	no. of matching peptldes MS/(MS/MS)	coverage (%)	sequenced peptides	score	MWt/ MWe (KDa)	pIt/pIe
1m	fast skeletal muscle troponin I	*Gadus morhua*	gi|20253043	de novo sequencing	2	9	SLILSIAAG (100% positives) IAAHLDR (100% positives)	106	18.9/19.0	8.7/8.7
2m	nucleoside diphosphate kinase B	*Merluccius capensis*	gi|1153705971	PMF + MS/MS	4/1	23	-.TFVAIKPDGVQR.G	110	14.2/14.1	5.7/7.4
3m	nucleoside diphosphate kinase B	*Merluccius capensis*	gi|1153705971	PMF + MS/MS	4/2	23	.TFVAIKPDGVQR K.MMLGETNPADSKPGSIR.G	115	14.2/14.1	5.7/6.7
4m	nucleoside diphosphate kinase B	*Merluccius capensis*	gi|1153705971	PMF + MS/MS	4/2	23	.TFVAIKPDGVQR K.MMLGETNPADSKPGSIR.G	207	14.2/9.4	5.7/6.7
5m	myosin light chain 2	*Theragra chalcogramma*	gi|111463956	PMF + MS/MS	13/5	48	K.EAFTIIDQNR.D K.GADPEDVIVAAFK.I K.LKGADPEDVIVAAFK.I K.DDLRDVLASMGQINVK.N K.EASGPINFTVFLTMFGEK.L	486	19.0/9.4	4.7/4.6
6m	myosin light chain 2	*Theragra chalcogramma*	gi|111463956	PMF + MS/MS	8/3	36	K.LKGADPEDVIVAAFK.I K.EFLQELLTTQCDR.F K.EASGPINFTVFLTMFGEK.L	165	19.0/13.8	4.7/4.6
7m	myosin light chain 2	*Theragra chalcogramma*	gi|111463956	PMF + MS/MS	11/3	48	K.EAFTIIDQNR.D K.GADPEDVIVAAFK.I K.EASGPINFTVFLTMFGEK.L	359	19.0/18.3	4.7/4.6
8m	myosin light chain 3	*Theragra chalcogramma*	gi|111463954	PMF + MS/MS	9/2	40	R.INFESFLPMLK.V K.RINFESFLPMLK.V	121	17.2/14.4	4.3/4.2
9m	myosin light chain 3	*Theragra chalcogramma*	gi|111463954	PMF+MS/MS	13/4	77	K.EAFTIIDQNR.D K.GADPEDVIVAAFK.I R.INFESFLPMLK.V R.VG DSQVAFSQVAD1MR.A	374	17.2/19.0	4.3/4.2
10m	adenylate kinase 1-2	*Epinephelus coioides*	gi|222033001	PMF + MS/MS	12/4	37	K.RLDLYVK.A K.IIFWGGPGSGK.G K.ATEPVIAFVEGR.G K.YGYTHLSSGDLLR.A	389	21.2/20.6	7.6/7.8
11m	myosin light chain 1	*Theragra chalcogramma*	gi|7673762	PMF + MS/MS	14/3	62	R.EAFGLFDR.V K.GTLDDWEGLR.V K.RVDFEGFLPMMQTIVNSPNK.G	311	21.2/21.2	4.7/4.7
12m	triosephosphate isomerase	*Lepisosteus osseus*	gi|146349397	PMF + MS/MS	7/2	29	K.GAFTGEISPAMIK.D R.HVFGESDELIGQK.V	231	24.3/22.7	5.9/7.6
13m	PDZ and LIM domain 7	*Epmephelus coioides*	gi|1222037993	PMF + MS/MS	7/3	15	K.FLTEIQSPR.Y K.DFSMPLTVSR.L R.EKFLTEIOSPR.Y	172	24.3/27.2	65/6.9

dx.doi.org/10.1021/jf201080t |J. Agric. Food Chem. 2011, 59, 7962–7977

Table 3. Continued

spot no.	identification	species	NCBI accession no.	identification method	no. of matching peptldes MS/(MS/MS)	coverage (%)	sequenced peptides	score	MWt/ MWe (KDa)	pIt/pIe
14m	fast skeletal muscle α-actin	*Gadus morhua*	gi|22654302	PMF + MS/MS	15/5	31	K.IIAPPER.K R.GYSFVTTAER.E K.QEYDEAGPSIVHR.K K.SYELPDGQVITIGNER.F K. DLYANN VLSGGTTM YPGI ADR.M	485	41.9/27.5	5.2/5.6
15m	fast skeletal muscle α-actin	*Gadus morhua*	gi|22654302	PMF + MS/MS	17/4	41	K.IIAPPER.K R.GYSFVTTAER.E K.SYELPDGQVITIGNER.F R.VAPEEHPTLLTEAPLNPK.A	422	41.9/25.9	5.2/5.3
16m	F-actin-capping protein subunit *β*	*Anoplopoma fimbria*	gi|1229366390	PMF + MS/MS	8/3	18	R.STLNEIYFGK.T K.LEVEANNAFDQYR.D R.KLEVEANNAFDQYR.D	232	30.5/28.3	5.5/5.3
17m	L-lactate dehydrogenase A chain	*Elegmops maclo*	gi|117433119	PMF + MS/MS	9/2	22	K.FIIPNIVK.Y K.LKGEVMDLQHGSLFLK.T	123	36.3/31.2	6.5/7.4
18m	glyceraldehyde 3-phosphate	*Gadus morhua*	gi|25939135	PMF + MS/MS	19/5	55	R.VPTPNVSWDLTVR.L K.LVTWYDNEFGYSNR.V R.SSIFDAGAGIALNDHFVK.L K.GILGYTEDQVVSTDFNGDI R.S K.VIHDNFGIVEGLMSTVHAITATQK.T	507	36.1/33.6	7.7/8.5
19m	glyceraldehyde 3-phosphate	*Gadus morhua*	gi|25939135	PMF+MS/MS	18/5	48	R.VPTPNVSVVDLTVR.L K.LVTWYDNEFGYSNR.V R.SSIFDAGAGIALNDHFVK.L K.GILGYTEDQVVSTDF NGDIR.S K.VIHDNFGIVEGLMSTVHAITATQK.T	648	36.1/33.0	7.7/8.2
20m	fructose-bis phosphate aldolase C	*Carassius auratus*	gi|11143277	de novo sequencing	2	5	QELAFATVTALR (91% positives) ENANVLAR (19% positives)	132	39.5/36.3	6.4/8.3
21m	creatine kinase	*Gadus morhua*	gi|113274539	PMF + MS/MS	14/4	45	K.GFTLPPHNSR.G K.LSIEALATLSGEFK.G K.TFLVWVNEEDHLR.V R.GTGGVDTASVGGVFDISNADR.L	462	28.9/37.5	8.9/7.3
22m	creatine kinase muscle isoform 2	*Chaenocephalus aceratus*	gi|131322099	PMF + MS/MS	11/3	23	K.LSVEALTSLDGEFK.G R.LGSSE VAQVQLWDGVK.L R.GTGGVDTASVGGVFDISNADR.L	454	42.7/39.2	6.4/7.3
23m	fast skeletal muscle α-actin	*Gadus morhua*	gi|22654302	PMF + MS/MS	13/3	35	R.GYSFVTTAER.E R.AVFPSIVGRPR.H KSYELPDGOVITIGNER.F	319	41.9/39.6	5.2/6.0

dx.doi.org/10.1021/jf201080t |J. Agric. Food Chem. 2011, 59, 7962–7977

Table 3. Continued

spot no.	identification	species	NCBI accession no.	identification method	no. of matching peptldes MS/(MS/MS)	coverage (%)	sequenced peptides	score	MWt/ MWe (KDa)	pIt/pIe
24m	fast skeletal muscle α-actin	*Gadus morhua*	gi|22654302	PMF + MS/MS	16/2	44	R.GYSFVTTAER.E K.SYELPDGQVITIGNER.F	297	41.9/40.2	5.2/5.8
25m	fast skeletal muscle α-actin	*Gadus morhua*	gi|22654302	PMF + MS/MS	19/3	39	R.AVFPSIVGRPR.H K.IWHHTFYNELR.V KSYELPDGOVITIGNER	327	41.9/42.0	5.2/5.2
26m	unnamed protein product (similar to enolase 1)	*Tetraodon nigroviridis*	gi|147210309	PMF + MS/MS	10/2	26	K.IIIGMDVAASEFYR.S K.DATNVGDEGGFAPNILENNEALELLK.S	157	47.1/46.3	6.0/6.4
27m	α-enolase-1	*Amia calva*	gi|111999247	PMF + MS/MS	10/4	25	R.YITPDQLADLYK.G K.IVIGMDVAASEFYK.D R.AAVPSG ASTGIYEALELR.D K.LAMQEFMILPVGASSFK.E	439	39.1/48.3	5.5/6.1
28m	hypothetical protein Zgc:66097 (similar to myosin binding prortein C)	*Danio rerio*	gi|141054699	de novo sequencing	1	2	EWFTVLEHFHR (100% positives)	92	55.9/74.8	6.3/6.4
29m	nucleoside diphosphate kinase	*Merluccius capensis*	gi|1153705971	PMF + MS/MS	2/2	23	-.TFVAIKPDGVQR.G K.MMLGETNPADSKPGSIR.G	174	14.1/15.1	5.7/6.6

[a] Spots of interest were identified by MS as described under Materials and Methods. Protein spot numbers (a) refer to numbered spots in Figure 1. For each spot, different parameters clarifying protein identification by MS are indicated (accession number; identification method (PMF, protein mass fingerprint; or MS/MS, protein sequencing); number of matching peptides in MS mode (fingerprinting) and MS/MS mode (sequencing); % sequence coverage; sequence of sequenced peptides, mascot score, theoretical and experimental protein mass (MWt and MWe), theoretical and experimental protein isoelectric point (pIt and pIe).

dx.doi.org/10.1021/jf201080t |J. Agric. Food Chem. 2011, 59, 7962–7977

explain the strongest oxidative vulnerability of the most acidic isoforms of phosphoglycerate mutase (spot 11s) and glyceraldehyde 3-phosphate dehydrogenase (spot 15s), indicating that protein phosphorylation may play an important role in activating metal-catalyzed protein oxidation.

Protein Oxidation in the Myofibril Protein Fraction. The incubation of myofibril proteins with Fe(II)/ascorbate caused important changes in the overall protein pattern (Figure 3A,B). Table 4 shows the quantitative changes in spot intensity for the proteins that exhibited significant appearance/disappearance upon MCO. Protein fold, oxidation fold, and oxidation index were calculated as described above. Protein spots 5m, 7m, and 9m, which appeared in the oxidized samples, were not observed in the 2-DE gels of the control samples (Figure 3A,B and Table 4). The protein folds were calculated by including "empty" spots as described under Materials and Methods. Protein spots 5m and 7m were both identified to be myosin light chains (MLC) 2, having, respectively, a smaller and larger size than the original MLC2 isoform present in nonoxidized samples (spot 6m). The experimental protein masses (MWe) for 5m, 6m, and 7m spots were 9.4, 13.8, and 18.3 kDa, respectively (Table 3). The theoretical molecular weight (MWt) of the MLC2 isoform identified is 19.0 kDa, which is similar to the experimental mass of the protein oxidation product 7m (18.3 kDa) and not to the experimental mass of original MLC2 isoform present in nonoxidized samples (13.8 kDa). The contradictory observations might be explained by the fact that the molecular weight of MLC2 isoforms ranges between 14 and 19.5 kDa depending on the fish species[34] and that the identification was assigned to MLC2 of a fish species different from the Atlantic cod investigated in the present study. It should be noted that the protein sequence for many fish species is still not available in the databases. Protein spot 9m was identified to be MLC3. It exhibited a slightly larger size than the original isoform of MLC3 present in nonoxidized samples (spot 8m). FTSC staining indicated the presence of carbonylation for spots 5m, 7m, and 9m (Figure 3D). As a consequence, we hypothesize that these proteins are oxidation byproducts of myosin. Previous studies have revealed that the myosin heavy chain (MHC) is almost completely lost under oxidative conditions (storage or forced oxidation with pro-oxidant agents), whereas the content of myosin light chains is significantly increased.[35] Our results suggest that the byproducts generated by oxidative degradation of MHC or MLC are partially carbonylated.

MCO also induced the formation of a degradation product of nucleoside diphosphate kinase B, protein spot 29m, which has been also observed in the sarcoplasmic fraction. This oxidative product of NDK B did not exhibit significant carbonylation (Figure 3D and Table 4). Actin (spot 25m) was also found to be degraded by oxidation because several protein spots identified as actin (14m, 15m, 23m, and 24m) were exclusively observed in Fe(II)/ascorbate-treated samples. The experimental masses found for protein spots 14m (27.5 kDa) and 15m (25.9 kDa) were significantly smaller than the theoretical mass of the original actin (MW = 41.9 kDa) and are therefore suggested to be oxidation-mediated backbone cleavage products of actin. This finding is in agreement with previous investigations that reported an important protein fragmentation of human serum albumin under MCO induced by copper/hydrogen peroxide treatment.[36] Spots 23m and 24m had a similar size to actin, but they exhibited a considerably more basic isoelectric point (Table 3). We do not have an explanation for this because none of these degradation byproducts of actin showed any substantial carbonylation.

Myofibril proteins in the samples that were not submitted to ferrous oxidation showed significant levels of carbonylation for protein spots 19m (glyceraldehyde 3-phosphate dehydrogenase), 21m and 22m (creatine kinase), and 25m (fast skeletal muscle α-actin) (Figure 3C). Actin was one of the most oxidized and abundant proteins in control myofibril proteins (Figure 3A,C). The exposure of myofibril proteins to the Fe(II)/ascorbate increased the carbonylation level for actin (spot 25m) approximately 6-fold (Figure 3D and Table 5). In the presence of Fe(II)/ascorbate, oxidation levels were also increased from 3.8- to 7.3-fold for other proteins that presented detectable oxidation background in the control samples (spots 19m, 21m, and 22m). Protein spots identified as degradation products of myosin light chain (spots 5m, 7m, and 9m) exhibited important oxidation levels, and their oxidation indices reached elevated values, ranging between 26.3- and 50.3-fold. MLC1 (protein spot 11 m), which was present in both controls and oxidized samples, also showed a significant increase in the carbonylation level (oxidation index = 35.9). The oxidation levels of protein spots 3m and 4m, identified as nucleoside diphosphate kinase B, also increased considerably upon oxidation, with oxidation indices between 31 and 42. Oxidation indices of 25.9 and 37.3, respectively, were observed for protein spots 26m (unnamed protein product similar to enolase-1) and 28m (hypothetical protein Zgc:66097 similar to myosin binding protein). MCO also resulted in elevated oxidation indices (4.5−11.8) for protein spots 19m (glyceraldehyde 3-phosphate dehydrogenase), 21m (creatine kinase), 22m (creatine kinase), and 27m (α-enolase-1). These results expand previous studies that indicated the elevated propensity of nucleoside diphosphate kinase, actin, creatine kinase, myosin light chains 1 and 2, and myosin heavy chain to undergo carbonylation during the frozen storage of rainbow trout fillets.[23]

Previously, it was reported that myosin may undergo either cross-linking through disulfide bond formation[37,38] or fragmentation[39] under oxidative conditions. The degradation of fish myosin heavy chain has been documented in the presence of heme proteins[38,40] and during a prolonged ripening period.[41] We have found that the Fe(II)/ascorbate treatment considerably enhances carbonylation of important structural proteins in fish muscle, mainly actin and myosin. Moreover, degradation products of actin and myosin are generated, and some of them exhibit increased carbonylation levels.

To illustrate the contribution of proteins of similar functions to the overall protein abundance and oxidation patterns in cod muscles, we have divided proteins into six groups: (1) structural; (2) energy homeostasis; (3) glycolysis and carbohydrate metabolism; (4) redox regulation; (5) other; and (6) unknown. Figure 4 depicts the distribution of protein abundance in the specified groups (panel A) and the distribution of carbonyl levels found in oxidized proteins in the specified groups (panel B). The distribution of the protein abundance was calculated on the basis of the total intensity of Sypro Ruby-stained spots found within the same biological function group by the intensity of all protein spots in oxidized samples. Likewise, the level of protein carbonylation of proteins classified to the same functional group was obtained by summing the FTSC intensity of corresponding spots and relating it to the total FTSC intensity of all spots in oxidized samples. The six identified proteins with structural functions representing 17.5% of the total spot intensity accounted for more than half of the total carbonylation signal measured in Fe(II)/ascorbate-treated samples. On the contrary, proteins with catalytic functions in glycolysis and carbohydrate metabolism,

Table 4. Significant Changes in Protein Spot Intensity Observed in the Myofibril Protein Fraction from Cod Muscle upon Ferrous-Catalyzed Oxidation

spot no.	identification	NCBI accession no.	protein fold[a]	exclusive presence in ferrous-treated samples[b]	detectable levels of oxidation[c]
3m	nucleoside diphosphate kinase B	gi|158705971	1.80 ± 0.02**		X
5m	myosin light chain 2	gi|11463956	3.05 ± 0.30***	X	X
7m	myosin light chain 2	gi|11463956	3.50 ± 0.50**	X	X
9m	myosin light chain 3	gi|11463954	3.18 ± 0.45**	X	X
14m	fast skeletal muscle α-actin	gi|22654302	4.18 ± 1.12*	X	
15m	fast skeletal muscle α-actin	gi|22654302	8.12 ± 0.70***	X	
16m	F-actin-capping protein subunit β	gi|229366390	1.94 ± 0.11*		
23m	fast skeletal muscle α-actin	gi|22654302	7.80 ± 0.80***	X	
24m	fast skeletal muscle α-actin	gi|22654302	5.17 ± 0.19***	X	
26m	unnamed protein product (similar to enolase 1)	gi|47210809	0.72 ± 0.039*		X
28m	hypothetical protein Zgc:66097 (similar to myosin binding protein C)	gi|41054699	0.69 ± 0.061*		X
29m	nucleoside diphosphate kinase B	gi|158705971	10.30 ± 1.05***	X	

[a] Protein fold between myofibril proteins subjected to ferrous-catalyzed oxidation and those not incubated with ferrous (controls) are calculated from quantification of Sypro Ruby-stained 2-DE gels. For those proteins exclusively found in the ferrous-treated samples, protein folds were calculated on the basis of the increment of Sypro Ruby intensity over the Sypro Ruby background. Significant differences were detected in the protein levels of nonoxidized myofibril proteins and those oxidized with the ferrous system for $p < 0.05$ (*), $p < 0.005$ (**) or $p < 0.0005$) (***). [b] Spots marked with X were exclusively found in the ferrous-treated myofibril proteins. [c] Spots marked with X showed carbonylation in ferrous-treated myofibril proteins.

Table 5. Quantification of Ferrous-Induced Oxidation of the Myofibril Fraction Proteins from Cod Muscle

spot no.	identification	NCBI accession no.	protein fold[a]	oxidation fold[b]	oxidation index[c]
3m	nucleoside diphosphate kinase B	gi|158705971	1.80 ± 0.03	76.0 ± 13.1**	42.1
4m	nucleoside diphosphate kinase B	gi|158705971	1.00 ± 0.10	31.2 ± 4.1***	31.2
5m	myosin light chain 2	gi|11463956	3.05 ± 0.30	80.3 ± 6.8***	26.3
7m	myosin light chain 2	gi|11463956	3.50 ± 0.50	161.5 ± 10.0***	46.2
9m	myosin light chain 3	gi|11463954	3.18 ± 0.45	160.1 ± 42.7**	50.3
11m	myosin light chain 1	gi|7678762	1.15 ± 0.17	41.4 ± 2.9***	35.9
19m	glyceraldehyde 3-phosphate dehydrogenase	gi|25989185	0.97 ± 0.02	8.5 ± 2.0**	8.8
21m	creatine kinase	gi|13274539	0.93 ± 0.03	7.3 ± 1.3**	7.8
22m	creatine kinase muscle isoform 2	gi|31322099	0.83 ± 0.09	3.8 ± 1.1*	4.5
25m	fast skeletal muscle α-actin	gi|22654302	0.97 ± 0.09	6.2 ± 0.7***	6.4
26m	unnamed protein product (similar to enolase 1)	gi|47210809	0.73 ± 0.04	18.8 ± 0.1***	25.9
27m	α-enolase-1	gi|11999247	0.74 ± 0.08	8.8 ± 0.7***	11.8
28m	hypothetical protein Zgc:66097 (similar to myosin binding protein C)	gi|41054699	0.69 ± 0.12	25.9 ± 6.3**	37.3

[a] Protein folds between myofibril proteins subjected to ferrous-catalyzed oxidation and those not incubated with ferrous (controls) are calculated from quantification of Sypro Ruby-stained 2-DE gels. For the proteins exclusively found in the ferrous-treated samples (spots 5, 7, and 9), protein folds were calculated on the basis of the increment of Sypro Ruby intensity over the Sypro Ruby background. [b] Oxidation folds between myofibril proteins subjected to ferrous-catalyzed oxidation and those not incubated with ferrous (controls) are calculated from quantification of FTSC-stained 2-DE gels. Protein carbonylation levels between ferrous-treated myofibril proteins and those not treated (controls) were found to be significantly different at <0.05 (*), <0.005 (**), or <0.0005) (***). [c] Oxidation indices correspond to the oxidation fold normalized with the corresponding protein fold.

accounting for 33.4% of all spot intensity, contribute only 12% of the total oxidation signal measured (Figure 4). Proteins with biological function for energy homeostasis (31.9% of total spot intensity) also exhibited a relatively high oxidation level, accounting for 30% of total carbonyl level. These results point to the high susceptibility of structural proteins from fish muscle to oxidative degradation in the presence of ferrous ions. Detailed studies are required to establish the factors responsible of such oxidative instability. The low oxidative resistance of structural proteins might explain the poor texture-forming ability and water-holding capacity observed in products prepared from meat exhibiting signs of oxidation.[1] Xiong et al.[42] reported cross-linking of porcine myofibril proteins by incubation with a hydroxyl radical-producing system based on a ferrous Fenton-type reaction,

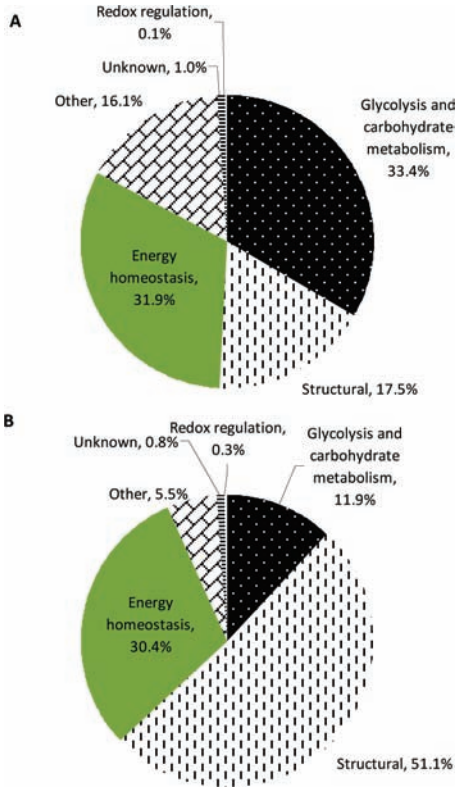

Figure 4. Distribution of protein abundance of all the identified proteins (A) and of carbonyl levels found in oxidized proteins (B) divided into different groups of proteins depending on their biological function. The distribution of the protein abundance was calculated by dividing the Sypro Ruby intensity of proteins found within the same biological function by the intensity of all identified proteins in oxidized samples. In a similar way, the proportion of carbonylation corresponding to proteins with similar function was obtained by dividing their FTSC intensity and the total FTSC intensity of all identified proteins in oxidized samples.

suggesting a relevant role of disulfide links into the polymerization of actin and myosin heavy chains.

In summary, an approach based on fluorescent-labeling on 2-DE gels instead of Western blotting was found to be advantageous in the identification of protein carbonylation. The fluorescent-labeling approach is less costly and time-consuming and avoids the loss of proteins during the transfer from the electrophoretic gel to the membrane. Our results show the existence of a detectable background carbonylation in cod muscle proteins. Additionally, we have shown that incubation of cod muscle proteins with Fe(II)/ascorbate significantly increases carbonylation levels of sarcoplasmic and myofibril proteins. Proteins displayed different susceptibilities to metal-catalyzed oxidation, indicating that this process is not a random event. Several protein isoforms most likely differing in phosphorylation state showed distinct oxidative patterns, suggesting an important role of phosphate groups in the activation of ferrous-catalyzed oxidation. Our results also show elevated susceptibility to oxidative degradation of the structural proteins myosin and actin, the integrity of which is essential for the textural characteristics of muscle tissues. More research evaluating protein oxidation under the presence of other pro-oxidant agents relevant in muscle-based food is needed to confirm the highly specific oxidation of proteins in the myofibril fraction and to identify the mechanism of interaction of these proteins with pro-oxidants.

AUTHOR INFORMATION

Corresponding Author

*E-mail: mpazos@iim.csic.es. Phone: +34 986 231930. Fax: +34 986 292762.

Funding Sources

Xunta de Galicia and the Spanish Ministry of Science and Innovation are gratefully acknowledged for the postdoctoral contract "Eduardo Parga Pondal" to M.P. and the financial support (AGL-2009-12374-C03-01), respectively. A Ph.D. grant for A.P.R. was funded by Alban Programme (European Union Programme of High Level Scholarships for Latin America). This work was supported (P.R., A.R.-W., and A.P.R.) by European sixth Framework Program Grant Proteomage LSHMCT-518230.

ACKNOWLEDGMENT

We are grateful to Andrea Maria Lorentzen for her excellent technical assistance.

REFERENCES

(1) Xiong, Y. L. Protein oxidation and implications for muscle food quality. In *Antioxidants in Muscle Foods*; Decker, E., Faustman, C., Eds.; Wiley-Interscience: New York, 2000; pp 85−111.

(2) Hultin, H. O. Oxidation of lipids in seafoods. In *Seafoods. Chemistry, Processing, Technology and Quality*; Shahidi, F., Botta, J. R., Eds.; Blackie Academic and Professional: Suffolk, U.K., 1994; pp 49−74.

(3) Frankel, E. N. *Lipid Oxidation*; Oily Press: Dundee, Scotland, 1998.

(4) Headlam, H. A.; Davies, M. J. Markers of protein oxidation: different oxidants give rise to variable yields of bound and released carbonyl products. *Free Radical Biol. Med.* **2004**, *36*, 1175–1184.

(5) Uchida, K. Histidine and lysine as targets of oxidative modification. *Amino Acids* **2003**, *25*, 249–257.

(6) Amici, A.; Levine, R. L.; Tsai, L.; Stadtman, E. R. Conversion of amino-acid residues in proteins and amino-acid homopolymers to carbonyl derivatives by metal-catalyzed oxidation reactions. *J. Biol. Chem.* **1989**, *264*, 3341–3346.

(7) Miyata, T.; Inagi, R.; Asahi, K.; Yamada, Y.; Horie, K.; Sakai, H.; Uchida, K.; Kurokawa, K. Generation of protein carbonyls by glycoxidation and lipoxidation reactions with autoxidation products of ascorbic acid and polyunsaturated fatty acids. *FEBS Lett.* **1998**, *437*, 24–28.

(8) Suman, S. P.; Faustman, C.; Stamer, S. L.; Liebler, D. C. Proteomics of lipid oxidation-induced oxidation of porcine and bovine oxymyoglobins. *Proteomics* **2007**, *7*, 628–640.

(9) Levine, R. L.; Williams, J. A.; Stadtman, E. P.; Shacter, E.; Lester, P. [37] Carbonyl assays for determination of oxidatively modified proteins. In *Methods in Enzymology*; Academic Press: New York, 1994; Vol. 233, pp 346−357.

(10) Matthijssens, F.; Braeckman, B. P.; Vanfleteren, J. R. Evaluation of different methods for assaying protein carbonylation. *Curr. Anal. Chem.* **2007**, *3*, 93–102.

(11) Fagan, J. M.; Sleczka, B. G.; Sohar, I. Quantitation of oxidative damage to tissue proteins. *Int. J. Biochem. Cell Biol.* **1999**, *31*, 751–757.

(12) Nakamura, A.; Goto, S. Analysis of protein carbonyls with 2, 4-dinitrophenyl hydrazine and its antibodies by immunoblot in two-dimensional gel electrophoresis. *J. Biochem.* **1996**, *119*, 768–774.

(13) Mirzaei, H.; Regnier, F. Affinity chromatographic selection of carbonylated proteins followed by identification of oxidation sites using tandem mass spectrometry. *Anal. Chem.* **2005**, *77*, 2386–2392.

(14) Yoo, B.-S.; Regnier, F. E. Proteomic analysis of carbonylated proteins in two-dimensional gel electrophoresis using avidin−fluorescein affinity staining. *Electrophoresis* **2004**, *25*, 1334–41.

(15) Mirzaei, H.; Regnier, F. Enrichment of carbonylated peptides using girard p reagent and strong cation exchange chromatography. *Anal. Chem.* **2006**, *78*, 770–778.

(16) Chaudhuri, A. R.; de Waal, E. M.; Pierce, A.; Van Remmen, H.; Ward, W. E.; Richardson, A. Detection of protein carbonyls in aging liver tissue: a fluorescence-based proteornic approach. *Mech. Ageing Dev.* **2006**, *127*, 849–861.

(17) Lindahl, G.; Lagerstedt, Å.; Ertbjerg, P.; Sampels, S.; Lundström, K. Ageing of large cuts of beef loin in vacuum or high oxygen modified atmosphere − effect on shear force, calpain activity, desmin degradation and protein oxidation. *Meat Sci.* **2010**, *85*, 160–166.

(18) Tokur, B.; Polat, A. Myofibrillar and sarcoplasmic protein oxidation and degradation of thin-lipped gray mullet (*Liza ramada*) during refrigerated storage (4c). *J. Muscle Foods* **2008**, *21*, 102–118.

(19) Gatellier, P.; Kondjoyan, A.; Portanguen, S.; Sante-Lhoutelher, V. Effect of cooking on protein oxidation in n-3 polyunsaturated fatty acids enriched beef. Implication on nutritional quality. *Meat Sci.* **2010**, *85*, 645–650.

(20) Stagsted, J.; Bendixen, E.; Andersen, H. J. Identification of specific oxidatively modified proteins in chicken muscles using a combined immunologic and proteomic approach. *J. Agric. Food Chem.* **2004**, *52*, 3967–3974.

(21) Santé-Lhoutellier, V.; Engel, E.; Aubry, L.; Gatellier, P. Effect of animal (lamb) diet and meat storage on myofibrillar protein oxidation and in vitro digestibility. *Meat Sci.* **2008**, *79*, 777–783.

(22) Kjaersgard, I. V. H.; Jessen, F. Two-dimensional gel electrophoresis detection of protein oxidation in fresh and tainted rainbow trout muscle. *J. Agric. Food Chem.* **2004**, *52*, 7101–7107.

(23) Kjaersgard, I. V. H.; Norrelykke, M. R.; Baron, C. P.; Jessen, F. Identification of carbonylated protein in frozen rainbow trout (*Oncorhynchus mykiss*) fillets and development of protein oxidation during frozen storage. *J. Agric. Food Chem.* **2006**, *54*, 9437–9446.

(24) Baron, C. P.; Kjaersgard, I. V. H.; Jessen, F.; Jacobsen, C. Protein and lipid oxidation during frozen storage of rainbow trout (*Oncorhynchus mykiss*). *J. Agric. Food Chem.* **2007**, *55*, 8118–8125.

(25) Kinoshita, Y.; Sato, T.; Naitou, H.; Ohashi, N.; Kumazawa, S. Proteomic studies on protein oxidation in bonito (*Katsuwonus pelamis*) muscle. *Food Sci. Technol. Res.* **2007**, *13*, 133–138.

(26) Joseph, P.; Suman, S. P.; Mancini, R. A.; Beach, C. M. Mass spectrometric evidence for aldehyde adduction in carboxymyoglobin. *Meat Sci.* **2009**, *83*, 339–344.

(27) Bradford, M. M. A rapid and sensitive method for the quantitation of microgram quantities of protein utilizing the principle of protein−dye binding. *Anal. Biochem.* **1976**, *72*, 248–254.

(28) Rogowska-Wrzesinska, A.; Larsen, P. M.; Blomberg, A.; Gorg, A.; Roepstorff, P.; Norbeck, J.; Fey, S. J. Comparison of the proteomes of three yeast wild type strains: Cen.Pk2, fy1679 and w303. *Comp. Funct. Genomics* **2001**, *2*, 207–225.

(29) Gobom, J.; Nordhoff, E.; Mirgorodskaya, E.; Ekman, R.; Roepstorff, P. Sample purification and preparation technique based on nano-scale reversed-phase columns for the sensitive analysis of complex peptide mixtures by matrix-assisted laser desorption/ionization mass spectrometry. *J. Mass Spectrom.* **1999**, *34*, 105–116.

(30) Shevchenko, A.; Sunyaev, S.; Loboda, A.; Shevehenko, A.; Bork, P.; Ens, W.; Standing, K. G. Charting the proteomes of organisms with unsequenced genomes by MALDI-quadrupole time of flight mass spectrometry and blast homology searching. *Anal. Chem.* **2001**, *73*, 1917–1926.

(31) Kanner, J. Oxidative processes in meat and meat products quality implications. *Meat Sci.* **1994**, *36*, 169–189.

(32) Baron, C. P.; Refsgaard, H. H. F.; Skibsted, L. H.; Andersen, M. L. Oxidation of bovine serum albumin initiated by the Fenton reaction − effect of EDTA, *tert*-butylhydroperoxide and tetrahydrofuran. *Free Radical Res.* **2006**, *40*, 409–417.

(33) Stanley, N.; Stadler, N.; Woods, A. A.; Bannon, P. G.; Davies, M. J. Concentrations of iron correlate with the extent of protein, but not lipid, oxidation in advanced human atherosclerotic lesions. *Free Radical Biol. Med.* **2006**, *40*, 1636–1643.

(34) Ochiai, Y.; Kobayashi, T.; Watabe, S.; Hashimoto, K. Mapping of fish myosin light chains by two-dimensional gel electrophoresis. *Comp. Biochem. Physiol. Part B: Comp. Biochem.* **1990**, *95*, 341–345.

(35) Tironi, V. A.; Tomás, M. C.; Añón, M. C. Quality loss during the frozen storage of sea salmon (*Pseudopercis semifasciata*). Effect of rosemary (*Rosmarinus officinalis* L.) extract. *LWT−Food Sci. Technol.* **2010**, *43*, 263–272.

(36) Ramirez, D. C.; Mejiba, S. E. G.; Mason, R. P. Copper-catalyzed protein oxidation and its modulation by carbon dioxide − enhancement of protein radicals in cells. *J. Biol. Chem.* **2005**, *280*, 27402–27411.

(37) Ooizumi, T.; Xiong, Y. L. Biochemical susceptibility of myosin in chicken myofibryls subjected to hydroxyl radical oxidizing systems. *J. Agric. Food Chem.* **2004**, *52*, 4303–4307.

(38) Frederiksen, A. M.; Lund, M. N.; Andersen, M. L.; Skibsted, L. H. Oxidation of porcine myosin by hypervalent myoglobin: the role of thiol groups. *J. Agric. Food Chem.* **2008**, *56*, 3297–3304.

(39) Liu, G.; Xiong, Y. L. Electrophoretic pattern, thermal denaturation, and in vitro degestibility of oxidized myosin. *J. Agric. Food Chem.* **2000**, *48*, 624–630.

(40) Lund, M. N.; Luxford, C.; Skibsted, L. H.; Davies, M. J. Oxidation of myosin by haem proteins generates myosin radicals and protein cross-links. *Biochem. J.* **2008**, *410*, 565–574.

(41) Andersen, E.; Andersen, M. L.; Baron, C. P. Characterization of oxidative changes in salted herring (*Clupea harengus*) during ripening. *J. Agric. Food Chem.* **2007**, *55*, 9545–9553.

(42) Xiong, Y. L.; Park, D.; Ooizumi, T. Variation in the cross-linking pattern of porcine myofibrillar protein exposed to three oxidative environments. *J. Agric. Food Chem.* **2009**, *57*, 153–159.